Calibrating the K&C Material Model for Fiber Reinforced Concrete Structures

Duc-Kien Thai and Duy-Duan Nguyen

1 Introduction

Fiber reinforced concrete (FRC) has been widely used in construction. A number of studies concerning about structural behavior of FRC have been carried out. For numerical analysis approach, the problem comes from the fact that, while there have been numerous material models for conventional concrete, none of the model has been developed specifically for FRC structures. Actually, the need to simulate FRC structures is increasing. This requires the improvement of material models relevant to structural behavior of FRC under both static and dynamic load conditions, which is very urgent.

The commercial software, LS-DYNA, provides several material models for concrete such as Karagozian & Case Concrete (K&C) model (MAT#072r3), Winfrith Concrete (MAT#084), and Continuous Surface Cap (CSC) model (MAT#159). Among them, K&C model, which was initially proposed by Malvar et al. [7], has been widely chosen by researchers for simulation of FRC structures subjected to both static and dynamic loading conditions. Since the structural behavior of FRC is quite different from the conventional concrete, it is required to calibrate the input parameters using test data. Lin and his colleagues [4, 5] calibrated this material model for high performance and ultra-high performance fiber reinforced concrete. However, the most significant limitation in these works is lacking of tri-axial test data, which directly support the calibration of the input parameters of the K&C model. Moreover, none of the given calibration provided calibrated input parameters that are capable to modeling of FRC. This fact gives a strong motivation to conduct this study.

This paper presents the calibration of K&C model for simulating the structural behavior of FRC structures under different loading conditions. For this purpose, various experimental data on tension, compression, and high-rate behaviors of FRC

D.-K. Thai (✉) · D.-D. Nguyen
Department of Civil and Environmental Engineering, Sejong University, Seoul 05006, Korea
e-mail: thaiduckien@sejong.ac.kr

J. N. Reddy et al. (eds.), *ICSCEA 2019*, Lecture Notes in Civil Engineering 80,
https://doi.org/10.1007/978-981-15-5144-4_19

material using axial and tri-axial tests are used to calibrate the input parameters. Numerical simulations of single tests on compression and bending subjected to static loading and of a FRC beam under blast loading are carried out to illustrate the performance of the calibrated material model. It is shown that results induced by the calibrated material model proposed in this study are in good agreement with the experimental data.

2 Calibration of Material Model

2.1 Three Failure Surfaces

The K&C material model [7] is a three-invariant model, in which the three independent shear surfaces are the functions of the hydrostatic pressure, as shown in Fig. 1. These three failure surfaces are determined based on three specific points yield (Pt. 1), maximum (Pt. 2), and residual (Pt. 3) strengths on the typical stress-strain relationship of compression test of concrete, as presented in Fig. 2.

The yield strength surface $\Delta\sigma_y$, maximum strength surface $\Delta\sigma_m$, and residual strength surface $\Delta\sigma_r$ are expressed as the function of pressure as

$$\Delta\sigma_y = a_{0y} + \frac{p}{a_{1y} + a_{2y}p}; \Delta\sigma_m = a_0 + \frac{p}{a_1 + a_2 p}; \text{ and } \Delta\sigma_r = \frac{p}{a_{1f} + a_{2f}p} \quad (1)$$

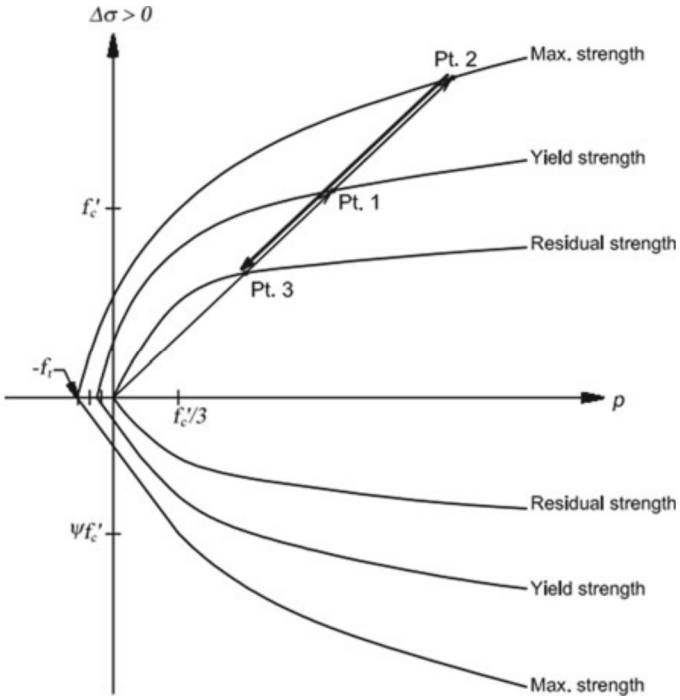

Fig. 1 Three failure surfaces in K&C model

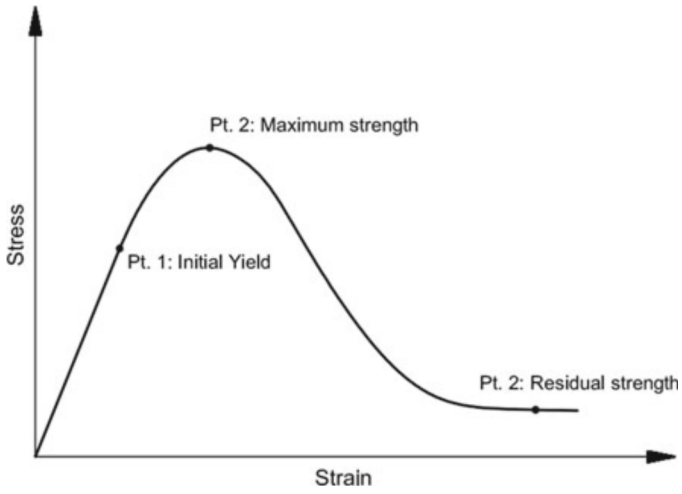

Fig. 2 Typical stress-strain curve of concrete

where $p = -(\sigma_1 + \sigma_2 + \sigma_3)/3$ is the pressure and a_{ij} are defined failure surfaces parameters, which are determined based on the tri-axial compression test data. The current stress limited by the deviatoric stresses is determined by mean of linear interpolation between the two surfaces, governed by the user-defined curve (η, λ).

The modified effective plastic strain is defined by the damage functions as

$$\lambda = \begin{cases} \int_0^{\overline{\varepsilon^p}} \dfrac{d\overline{\varepsilon^p}}{r_f\left(1 + p/r_f f_t\right)^{b1}} & \text{for } p \geq 0, \\ \int_0^{\overline{\varepsilon^p}} \dfrac{d\overline{\varepsilon^p}}{r_f\left(1 + p/r_f f_t\right)^{b2}} & \text{for } p < 0. \end{cases} \tag{2}$$

where $d\overline{\varepsilon^p}$ is the increment of effective plastic strain; r_f is the strain rate enhancement factor; f_t is the tensile strength of concrete; and b_1 and b_2 are the damage scaling parameters for the case of compression and tension, respectively.

To control the volumetric damage in tri-axial tension, a volumetric damage increment is added to the deviatoric damage whenever the stress path is close to the tri-axial tensile path. A ratio of $\left|\sqrt{3J_2}/p\right|$ is measured to be closeness to this path. The incremental damage now is multiplied by a factor f_d, given by

$$f_d = \begin{cases} 1 - \frac{\left|\sqrt{3J_2}/p\right|}{0.1}, & 0 \leq \left|\sqrt{3J_2}/p\right| < 0.1, \\ 0, & \left|\sqrt{3J_2}/p\right| \geq 0.1. \end{cases} \tag{3}$$

The modified effective plastic strain is incremented by

$$\Delta\lambda = b_3 f_d k_d \left(\varepsilon_v - \varepsilon_{v,yield}\right) \tag{4}$$

where b_3 is a damage parameter; k_d is the internal scalar multiplier; ε_v and $\varepsilon_{v,yield}$ are the volumetric strains at current and at yield, respectively.

The volumetric behaviour of this material model is governed by a pressure—volumetric strain curve, described by a tabulated compaction equation of state (EOS) function, expressed as

$$p = C(\varepsilon_v) + \gamma T(\varepsilon_v) E \tag{5}$$

where p is the current pressure; ε_v is the volumetric strain; $C(\varepsilon_v)$ is the tabulated pressure evaluated along the isotherm at 0.0 K; $T(\varepsilon_v)$ is the tabulated temperature-related parameter; γ is the specific heat ratio; and E is the internal energy.

2.2 Calibration of K&C Material Model

K&C model has total of 49 input parameters, which are defined by the user [6]. This section presents the calibration of input parameter for FRC based on the test data. The parameters on (1) failure surfaces, (2) damage function, (3) equation of state function, and (4) damage evolution are determined.

A series of compressive tests of FRC under active confining pressure, conducted by Gholampour and Ozbakkaloglu [1], is used. They provided the test data of axial stress-strain relationship with different levels of confining pressures of 0, 5, 10, 15, and 25 MPa. Two FRC mixes C50-1 and C100-1, corresponding to compressive strengths of 50 and 100 MPa, containing hooked fiber at a volume ratio of 1%, are selected for the purpose of this study.

A calibration procedure presented in Markovich et al. [8] is adopted in this process. Based on the stress-strain curves from the test data, the yield strengths, maximum strengths, and residual strengths are defined. Figure 3 shows the fitting curves for three independent strength surfaces. While, the calculated failure surface parameters for two different FRC mixes are summarized in Table 1.

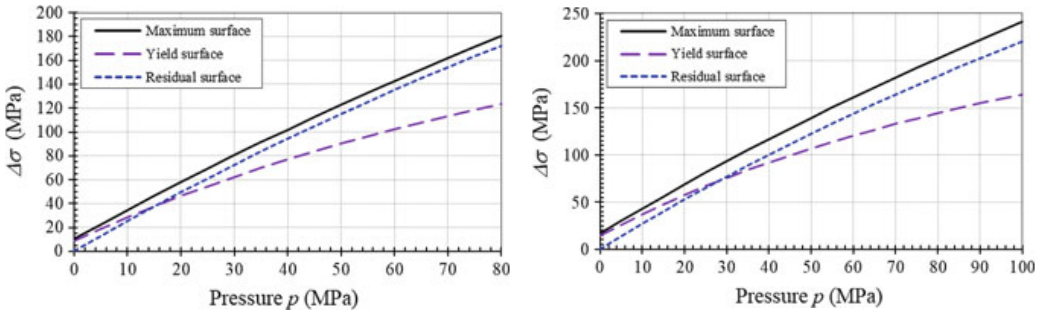

(a) C50-1 (a) C100-1

Fig. 3 Three independent strength surfaces

Table 1 Calculated failure surface parameters for FRC mixes

FRC mix	Failure surfaces parameters[a]							
	a_0	a_1	a_2	a_{0y}	a_{1y}	a_{2y}	a_{1f}	a_{2f}
C50-1	10.32	0.40,181	0.00085	8.46	0.47128	0.00281	0.38268	0.00102
C100-1	16.68	0.37027	0.00076	14.26	0.41249	0.00254	0.36272	0.00091

[a]The unit used for strength of FRC is MPa

Table 2 Defined rate enhancement factors

Strain rate	DIF	Strain rate	DIF
−1000	3.60	0	1.00
−500	3.09	0.00001	1.04
−100	1.90	0.0001	1.08
−53	1.33	0.001	1.12
−30	1.32	0.01	1.16
−20	1.31	0.1	1.21
−10	1.29	1	1.25
−1	1.25	10	1.30
−0.1	1.20	20	1.32
−0.01	1.15	30	1.60
−0.001	1.10	50	1.94
−0.0001	1.05	100	2.53
−0.00005	1.03	500	4.66
0	1.00	1000	6.07

The effect of strain-rate is taken into account by inputting the dynamic increment factor (DIF). In this study, the model of Sun et al. [10] is chosen for compression, whereas the model of Park et al. [9] is employed for tension. The input data for strain-rate enhancement factors are summarized in Table 2.

The damage function $\eta(\lambda)$ is a user-define function inputted as a series of 13 (η, λ) pairs. In this study, based on fitting with the test data, the calibrated input series of 13 (η, λ) pairs is presented in Table 3.

Table 3 Input parameters of damage function

Fair no.	λ	η	Fair no.	λ	η	Fair no.	λ	η
1	0	0.000	6	7.0e−4	0.920	11	5.0e−3	0.099
2	5.0e−6	0.200	7	8.0e−4	0.780	12	1.0e−0	0.001
3	1.0e−5	0.250	8	1.2e−3	0.520	13	1.0e−10	0.000
4	1.0e−4	0.660	9	1.8e−3	0.350			
5	6.0e−4	1.000	10	3.0e−3	0.180			

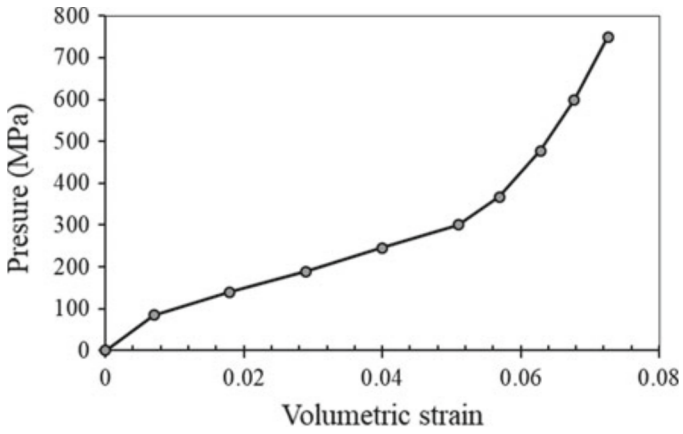

Fig. 4 Modified pressure versus volumetric strain curve for EOS

In LS-DYNA [6], the EOS used for MAT072r3 material model is the tabulated compaction equation of state, or EOS 8. Ten fairs of data points are required for input to define the equation of state function. Due to lack of test data on volumetric strain versus pressure of FRC, a modified curved from Unosson [11] is adopted in this study, as shown in Fig. 4.

3 Results and Discussion

3.1 Static Compression

To evaluate the performance of the calibrated model, a compression test conducted by Lee et al. [3] is selected and analyzed. The cylindrical specimen has diameter of 150 mm and length of 300 mm. The hooked fibers with aspect ratio of 63.6 and fiber content of 1% are used. The design compressive strength of the matrix is set to 50 MPa.

The solid element is used for FRC specimen model. The mesh size used in this study is 10 mm. Relevant boundary condition is applied to the specimen. This analysis uses the static option. Figure 5 shows the stress-strain curves of FEA and test results. Different values of damage parameter b_1 are varied to control the softening behavior of the compressive stress-strain curves. It is shown that the FEA curve fits well with the test curve at the damage parameter $b_1 = 0.53$. The comparison also emphasizes that the calibrated material model induces the compression behavior of FRC specimen accurately.

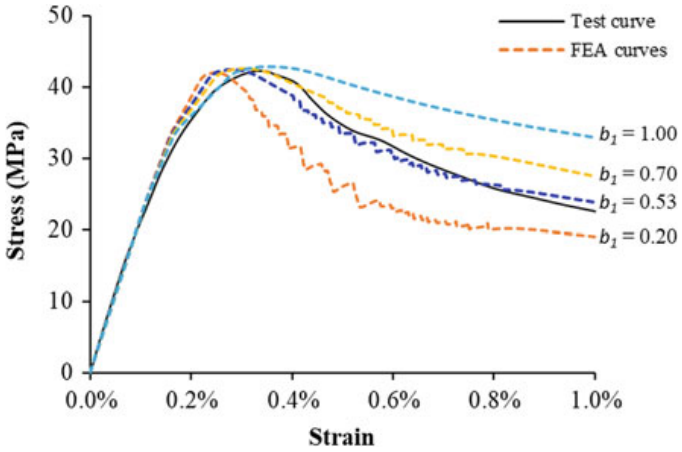

Fig. 5 Comparison of stress-strain curves

3.2 Blast Loading on FRC Beam

The dynamic performance of the calibrated model is also evaluated by simulating the FRC beam subjected to blast loading conducted by Lee et al. [2]. The specimen has section dimensions of 125 mm × 250 mm, and the length of 2438 mm, as shown in Fig. 6. Two longitudinal bars with diameter of 19.1 mm are installed in the tension face of the beam. Hooked fibers with content of 1% and aspect ratio of 60 were used in the test. Other detailed information of the test can be seen in Lee et al. [2]. A blast-like loading, which was generated using the shock tube system installed in the University of Ottawa, is adopted in this numerical analysis in terms of pressure-time history.

Solid elements are used for modelling of the FRC beam, whereas beam elements are utilized for modelling of the rebars. The mesh size of the finite element model is approximate 10 mm. Relevant boundary conditions are applied to the specimen to describe the realistic reaction of the support system. The dynamic analysis solver is used in this case.

Table 4 compares the maximum mid-span displacement between the test and FEA results. The comparison shows that the FEA result agrees well with the test datum

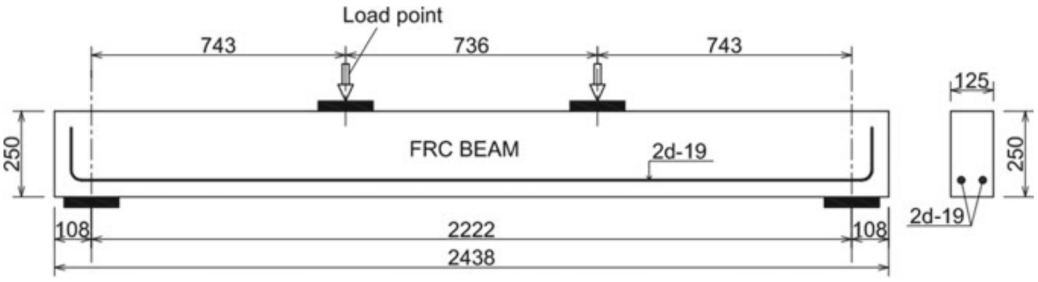

Fig. 6 Detail of specimen

Table 4 Comparison of maximum mid-span displacement

Method	Load	Max. mid-span displacement
Test	Blast No. 1	7.67
FEA	Blast No. 1	7.04
Difference	–	*8.2%*

since the difference of the maximum mid-span displacement is only 8.2%. It can be concluded that the FE modelling using the calibrated material model described in Sect. 2 can predict the dynamic behaviour of FRC beam under blast loading accurately.

4 Conclusion

A calibration of a material model implemented in LS-DYNA for analysing the static and dynamic behaviour of fiber reinforced concrete is presented in this paper. FE analyses of a FRC single specimen under static compressive loading and a FRC beam under blast-like loading are carried out to illustrate the performance of the calibration model. The results reveal that the FE analyses using the calibrated material model predict the structural behaviour of FRC components under both static and dynamic loading accurately. Thus, this calibrated material model can be used for further analyses of FRC structures under a wide range of loading rate.

Acknowledgements This work was supported by the National Research Foundation of Korea (NRF) grant funded by the Korea government (MSIT) (No. 2018R1C1B5086385).

References

1. Gholampour A, Ozbakkaloglu T (2018) Fiber-reinforced concrete containing ultra high-strength micro steel fiber under active confinement. Constr Build Mater 187:299–306
2. Lee JY, Shin HO, Yoo DY, Yoon YS (2018) Structural response of steel-fiber-reinforced concrete beams under various loading rates. Eng Struct 156:271–283
3. Lee SC, Oh JH, Cho JY (2015) Compressive behavior of fiber-reinforced concrete with end-hooked steel fibers. Materials 8:1442–1458
4. Lin X (2018) Numerical simulation of blast responses of ultra-high performance fibre reinforced concrete panels with strain-rate effect. Constr Build Mater 176:371–382
5. Lin X, Gravina RJ (2017) An effective numerical model for reinforced concrete beams strengthened with high performance fibre reinforced cementitious composites. Mater Struct 50(212):1–13
6. Livermore (2007) LS-DYNA keyword user's manual, version 971. California
7. Malvar LJ, Crawford JE, Wesevich JW, Simons D (1997) A plasticity concrete material model for DYNA3d. Int J Impact Eng 19(9):847–873
8. Markovich N, Kochavi E, Ben-Dor G (2011) An improved calibration of the concrete damage model. Finite Elem Anal Des 47:1280–1290

9. Park JK, Kim SW, Kim DJ (2017) Matrix-strength-dependent strain-rate sensitivity of strain-hardening fiber-reinforced cementitious composites under tensile impact. Compos Struct 162:313–324
10. Sun X, Zhao K, Li Y, Huang R, Ye Z, Zhang Y, Ma J (2018) A study of strain-rate effect and fiber reinforcement effect on dynamic behavior of steel fiber-reinforced concrete. Constr Build Mater 158:657–669
11. Unosson M (2000) Numerical simulations of penetration and perforation of high performance concrete with 75 mm steel projectile. In: FOA-R–00-01634-311–SE (ed.) Virginia